



REGULAR ARTICLE

Kinetics and mechanistic investigations on antiviral drug-valacyclovir hydrochloride by heptavalent alkaline permanganate

SURESH M TUWAR*  and ROHINI M HANABARATTI

Department of Chemistry, Karnatak Science College, Dharwad, Karnataka 580 001, India
E-mail: sm.tuwar@gmail.com

MS received 27 April 2021; revised 19 June 2021; accepted 21 June 2021

Abstract. Kinetics of Permanganate (MnO_4^-) oxidation of antiviral drug, valacyclovir hydrochloride (VCH) has been studied spectrophotometrically at a constant ionic strength of 0.1 mol dm^{-3} . The reaction exhibiting a 2:1 stoichiometry (MnO_4^- :VCH) has been studied over a wide range of experimental conditions. It was found that the rate enhancement was associated with an increase in concentrations of alkali, reductant and temperature. A plausible mechanism involving an intermediate Mn(VII)-VCH complex (C) was expected and rate law is derived accordingly. Calculated activation parameters also supported the anticipated mechanism.

Keywords. Heptavalent permanganate; Valacyclovir hydrochloride; Oxidation; Mechanism; Kinetics; Identification of product.

1. Introduction

Valacyclovir (VCH), a valine ester contains a guanine acyclic nucleoside. The two moieties are linked by a couple of alkyl oxygen bonds. Chemical name of VCH is L-valine-2-[(2-amino-1, 6-dihydro-6-oxo-9-hipurin-9-yl) methoxy] ethyl ester, also named as Valtrex. It is an L-valyl ester prodrug of the antiviral drug acyclovir that exhibits activity against herpes simplex virus types, (HSV-1), (HSV-2) and Varicella-zoster virus (VZV),¹ Scheme 1 reveals the structure of VCH.

In the mechanism of its action on herpes, acyclovir involves a highly selective inhibition of DNA replication virus, via enhanced uptake in herpes virus-infected cells and phosphorylation by viral thymidine kinase. VCH is rapidly converted to acyclovir and further phosphorylated to acyclovir triphosphate (ATP). The incorporation of ATP into the growing chain of viral DNA results in chain termination.^{2,3} The substrate specificity of ATP for viral, rather than cellular, DNA polymerase contributes to the specificity of the drug^{4,5} but VCH has side effects, like skin rash central nervous system effects with

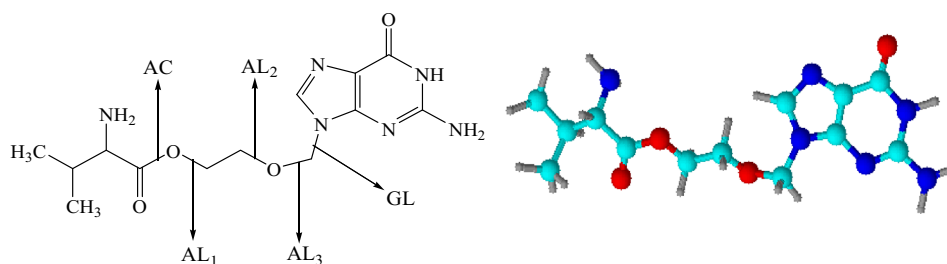
symptoms such as dizziness, confusion, headache numbness etc. These side effects may be due to the oxidative product of VCH.

Currently, COVID-19 (Coronavirus disease-2019) is treated with Remdesivir which is one of the expensive drugs. Recently, clinical trials are going on⁶ to treat the COVID-19 pandemic particularly SARS-CoV-2 infection with acyclovir which is formed in vivo by administering valacyclovir.

Oxidation by permanganate had earned more attention in green chemistry due to its versatile applications in several organic^{7,8} and inorganic^{9,10} redox reactions. The permanganate occurs in a few oxo-compounds¹¹ and has tetrahedral geometry with extensive p-bonding. The mechanistic pathways of MnO_4^- oxidation of organic substances like alcohols, aldehydes, alkenes and alkynes are depending upon the active species involved and its sensitivity to solvent, pH and other variables. Literature survey revealed that the dissolution studies,^{12,13} pharmacological data^{14,15} and a few methods are recommended for its analysis in pharmaceutical dosage forms by spectrophotometry,¹⁶ HPLC¹⁷ and RP-HPLC¹⁸ methods.

*For correspondence

Supplementary Information: The online version contains supplementary material available at <https://doi.org/10.1007/s12039-021-01969-4>.



2-[(2-amino-6,8di oxo-1,6,7,8-tetrahydro-9H-yl)methoxy]ethyl 2-amino-3-methylbutanoate

GL = Glycosidic Linkage

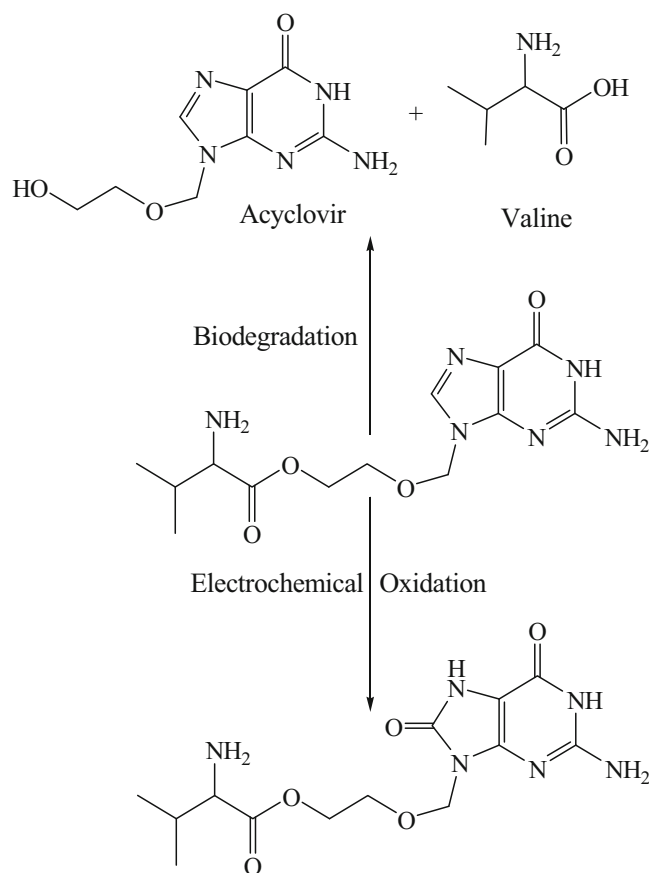
AL₁, AL₂ and AL₃ = Alkoxygen Bonds

AC = Acyloxygen Bonds

Scheme 1. Structure of valacyclovir

It is pertinent to mention that VCH hydrochloride undergoes acyl-oxygen bond cleavage in hydrolysis and biological systems to generate acyclovir^{19,20} and valine. Its electrochemical oxidation has led to the formation of imidazolone²¹ moiety without affecting the side chain (Scheme 2).

To the best of our knowledge and literature survey, there are no kinetic studies reported for oxidation of VCH using KMnO₄ in alkaline medium. Hence, the present investigation has been taken up to understand the mechanistic pathway of KMnO₄ oxidation and to identify the product obtained in this reaction.



2-[(2-amino-6,8-dioxo-1,6,7,8-tetrahydro-9H-yl)methoxy]ethyl 2-amino-3-methylbutanoate

Scheme 2. General mechanisms of oxidation of VCH

2. Experimental

2.1 Materials and reagents

All chemicals used were of AR grade and double distilled water was used throughout the study. VCH was procured from SD Fine Chemicals (India) with 98.0% purity. Further, its purity was checked by its melting point (198 °C) and GC-MS.

A stock solution of VCH was prepared by dissolving an appropriate quantity of sample in double-distilled water. The permanganate solution was prepared by dissolving the required amount of KMnO_4 crystals in distilled water and standardized against sodium oxalate.^{22,23} In addition, it is well-preserved in an amber glass bottle to avoid degradation due to exposure to sunlight and is characterized by a spectrophotometer. Potassium manganate (K_2MnO_4) solution was prepared as follows; an aqueous solution of KMnO_4 was heated to boiling > 100 °C in alkali. A green solution of K_2MnO_4 formed and was characterized by its visible spectrum at 608 nm ($\epsilon = 1530 \pm 100 \text{ dm}^3 \text{ mol}^{-1} \text{ cm}^{-1}$) (Figure 1). Further, it was used to verify the product effect on the rate of reaction.

2.2 Kinetic analysis

Kinetic analyses were carried out with $[\text{VCH}] > [\text{MnO}_4^-]$, supporting pseudo-first-order condition by

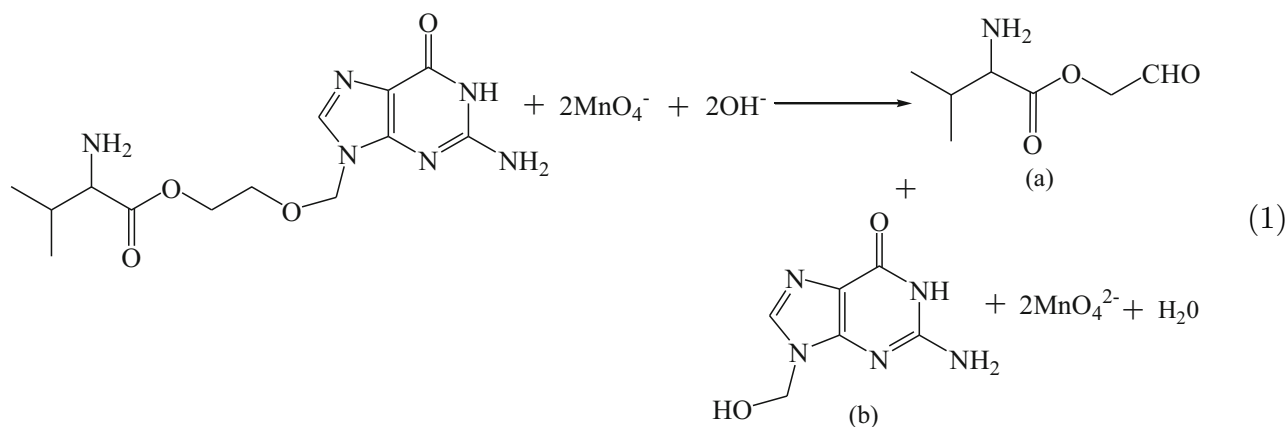
wavelength. The reaction was initiated by mixing previously thermostated MnO_4^- and VCH solutions, which also contained necessary concentrations of KOH and KNO_3 to maintain constant alkali and ionic strength respectively in the reaction.

Obedience to Beer's law for permanganate at 526 nm had been previously confirmed, giving $\epsilon = 2241 \pm 30 \text{ dm}^3 \text{ mol}^{-1} \text{ cm}^{-1}$ (Lit. value = $2200 \text{ dm}^3 \text{ mol}^{-1} \text{ cm}^{-1}$). Since, the first-order plots, $\log_{10}(\text{Abs.})$ versus Time were found to be linear up to 80% of the reaction, the rate constants, k_{obs} were calculated from the slopes of such plots for various experimental conditions. The experimental results were reproducible within $\pm 5\%$.

3. Results and Discussion

3.1 Stoichiometry and product analysis

Different sets of reaction mixtures containing varying ratios of $[\text{VCH}]$ to $[\text{MnO}_4^-]$ at constant ionic strength, 0.1 mol dm^{-3} in presence of constant $[\text{OH}^-]$ and $[\text{NO}_3^-]$ were kept for 24 h. in an inert atmosphere. The unreacted $[\text{MnO}_4^-]$ in every case was determined spectrophotometrically at 526 nm. The results indicate a 1:2 ($\text{VCH}:\text{MnO}_4^-$) stoichiometry as shown in Eqn. (1). MnO_4^{2-} as a reduction product was identified by measuring its optical density at 608 nm.



following absorption of MnO_4^- at its λ_{max} , 526 nm with a 1 cm quartz cell in Specord-200 plus spectrophotometer set up with a Peltier accessory as a function of time at 298 K unless otherwise stated. Prior to the reaction, it was confirmed that there is no interference from the other reagents at this

The oxidation products of VCH were evident for formylmethyl 2-amino-3-methylbutanoate and 2-amino-9-(hydroxymethyl)-1H-purin-6(9H)-one. After completion of the reaction, the solution was subjected to TLC for separation of components. It gave two spots with reference to VCH, which

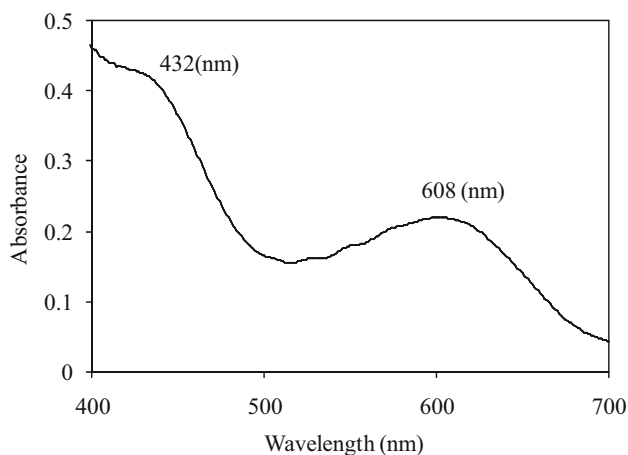


Figure 1. The spectrum of Potassium manganate (K_2MnO_4) in an aqueous alkaline medium at 298 K $[K_2MnO_4] = 1.0 \times 10^{-4} \text{ mol dm}^{-3}$ $[OH^-] = 0.05 \text{ mol dm}^{-3}$

confirmed the established products. Further, the formation of aldehyde was identified by spot test.²⁴

In addition, the solution was analyzed by LC-ESI-MS for mass evidence of the expected products. After completion of the reaction, it was treated with 50% methanol followed by acidification with HCl and 3% acetonitrile and 1% formic acid to make the solution in a positive ion mode. The solution was subjected at the rate of 5 $\mu\text{L}/\text{min}$ with retention time 0.51–0.98 s in the applied voltage of 30 kV with a glass microsyringe. The nitrogen gas was used as a nebulizer. The LC-ESI-MS spectra exhibited, m/z peak at 159 and 181 which are expected for formylmethyl 2-amino-3-methylbutanoate (a) and 2-amino-9-(hydroxymethyl)-1H-purin-6(9H)-one (b) respectively (Figure 2).

3.2 Reaction orders

The reaction orders were calculated from the slopes of plot, $\log_{10}k_{\text{obs}}$ versus \log_{10} (concentration) for varying [VCH] and $[OH^-]$ in turn keeping all other reactant conditions constant. Since the first-order plots were linear up to 80% completion of the reaction, the basic rate methods were used for determining the order of reactive species.

3.3 Influence of [permanganate]

Effect of $[MnO_4^-]$ on the rate of reaction was studied by varying the $[MnO_4^-]$ from 4.0×10^{-5} to $4.0 \times 10^{-4} \text{ mol dm}^{-3}$ at constant ionic strength by keeping all other conditions constant (Table 1). It was

found that k_{obs} values were constant for different $[MnO_4^-]$ and also found to be linear and parallel in pseudo-first-order plots. The order in $[MnO_4^-]$ was well-thought-out to be unity.

3.4 Influence of [VCH]

Effect of VCH on rate was studied by varying its concentration between 8.0×10^{-4} and $8.0 \times 10^{-3} \text{ mol dm}^{-3}$ by keeping other conditions constant (Table 1). It had been noticed that k_{obs} values increased with increasing [VCH]. The order in [VCH] was calculated from the plot of $\log_{10} k_{\text{obs}}$ versus \log_{10} [VCH] and was found to be a positive fraction (0.4).

3.5 Influence of $[OH^-]$

Effect of alkali on rate was studied by varying the $[OH^-]$ between 1.0×10^{-2} and $1.0 \times 10^{-1} \text{ mol dm}^{-3}$ by keeping other conditions constant at 298 K. It was observed that k_{obs} values were increased with an increase in $[OH^-]$ (Table 1). The order in $[OH^-]$ was calculated from the plots of $\log_{10} k_{\text{obs}}$ versus \log_{10} $[OH^-]$ and was found to be a positive fraction (0.4).

3.6 Influence of ionic strength (I) and dielectric constant of the medium (D)

The effect of ionic strength on rate was carried out by varying the $[KNO_3]$ between 0.05 and 0.6 mol dm^{-3} and keeping all other conditions constant (Table 2). It was observed that the added salt had no effect on the rate.

The effect of change in the dielectric constant of the medium on the reaction rate was studied by using different compositions (v/v) of t-butanol and water.²⁵ As 'D' decreases k_{obs} values decreased (Table 2). The dielectric constants of their different compositions were calculated by considering their D in pure form using the equation:

$$D = D_1V_1 + D_2V_2$$

where V_1 and V_2 are volume fractions and D_1 and D_2 are dielectric constants of water and t-butanol as 78.5 and 10.5, respectively at 298 K. Prior to the reaction, it was confirmed the inertness of the solvent with oxidant and other components of the reaction mixture.

3.7 Influence of initially added product

Effect of initially added product MnO_4^{2-} on the rate of reaction was verified between the series of 1.0×10^{-5}

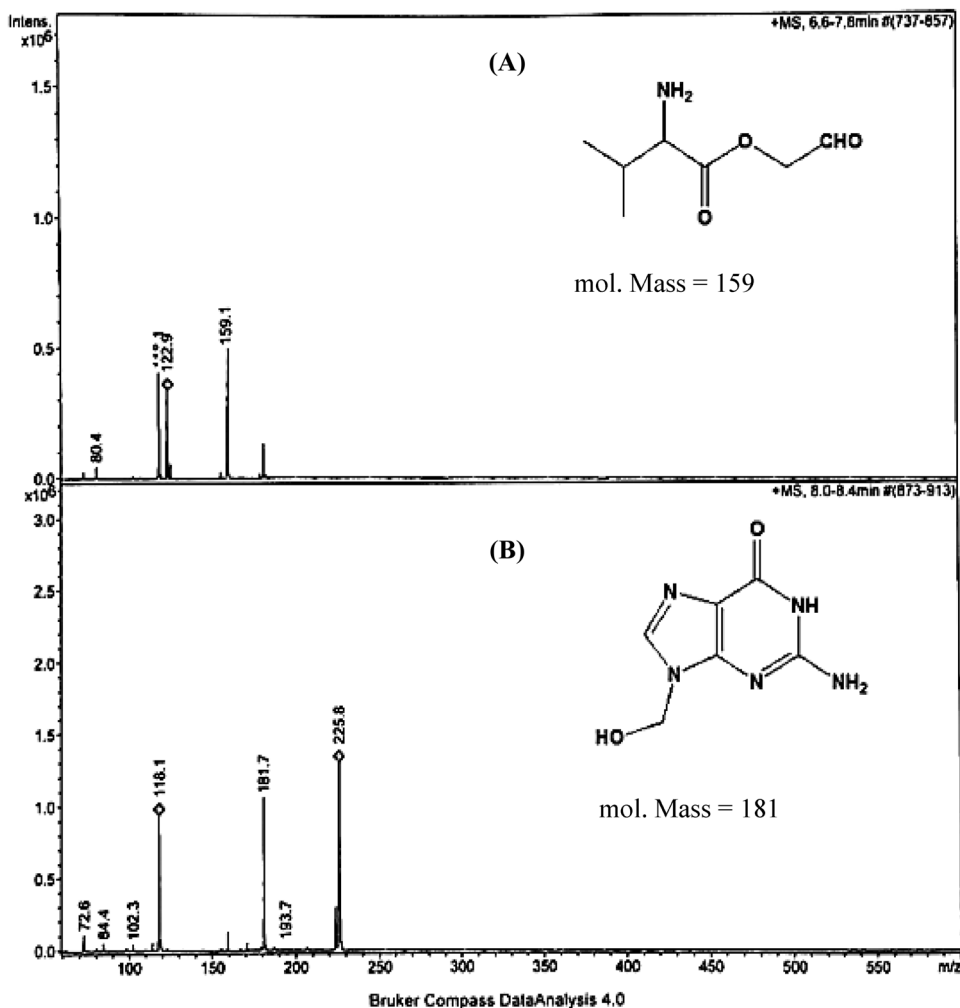


Figure 2. LC-ESI-MS (+) spectra of VCH products

and $1.0 \times 10^{-4} \text{ mol dm}^{-3}$ at 298 K by keeping all other conditions constant. The results indicate that the added product did not affect the rate.

3.8 Polymerization study

In the present study MnO_4^- is one equivalent oxidant in alkali. Hence, the reaction may proceed via free radical formation. In view of this, acrylonitrile was used as a free radical scavenger and tested in the reaction mixture as follows; the reaction mixture was mixed with acrylonitrile monomer and kept for 24 h in O_2 and CO_2 free atmosphere. A copious precipitation was formed on diluting the reaction mixture with methanol, indicating the intervention of free radicals in the reaction.

The experiment of either MnO_4^- or VCH with acrylonitrile alone did not induce the polymerization under similar condition as those induced with reaction

mixture. Initially added acrylonitrile also decreased the rate, indicating a free radical intervention.

3.9 Influence of temperature

By keeping constant conditions of the reaction, the temperature was raised to 298, 303, 308, 313 and 318 K. The rise in temperature shows an increase in the rate of reaction and calculated k_{obs} values are presented in Table 3.

The activation parameters for the reaction are calculated by using linear regression analysis (also known as the method of least square). In generalized notation, the formula for the straight line is $y = ax + b$. The most tractable form of linear regression analysis assumes that values of the independent variables 'x' are known without error and that experimental error is manifested only in values of the

Table 1. Effect of variations of $[\text{MnO}_4^-]$, $[\text{VCH}]$ and $[\text{OH}^-]$ in the oxidation of VCH by alkaline permanganate at 298 K.

I = 0.1 mol dm ⁻³					
$10^4 \times [\text{MnO}_4^-]$ mol dm ⁻³	$10^3 \times [\text{VCH}]$ mol dm ⁻³	$[\text{OH}^-]$ Mol dm ⁻³	$10^3 \times k_{\text{obs}}$ (s ⁻¹)	$10^3 \times k_{\text{cal}}$ (s ⁻¹)	
0.4	3.0	0.05	2.63	2.12	
0.6	3.0	0.05	2.23	2.12	
1.0	3.0	0.05	2.72	2.12	
2.0	3.0	0.05	2.72	2.12	
3.0	3.0	0.05	2.16	2.12	
4.0	3.0	0.05	2.30	2.12	
2.0	0.8	0.05	1.18	1.11	
2.0	1.5	0.05	1.63	1.59	
2.0	2.0	0.05	1.89	1.82	
2.0	3.0	0.05	2.24	2.12	
2.0	6.0	0.05	2.62	2.55	
2.0	8.0	0.05	2.89	2.70	
2.0	3.0	0.01	1.04	1.01	
2.0	3.0	0.03	1.87	1.79	
2.0	3.0	0.05	2.10	2.12	
2.0	3.0	0.07	2.35	2.30	
2.0	3.0	0.09	2.45	2.41	
2.0	3.0	0.10	2.50	2.45	

k_{cal} were calculated using $k = 3.18 \times 10^{-3} \text{ s}^{-1}$, $K_1 = 4.42 \text{ dm}^3 \text{ mol}^{-1}$, and $K_2 = 3.64 \times 10^3 \text{ dm}^3 \text{ mol}^{-1}$ at 298 K in rate eqn. (9).

Table 2. Effect of ionic strength (I) and dielectric constant (D) on the oxidation of VCH by alkaline permanganate at 298 K.

$[\text{MnO}_4^-] = 2.0 \times 10^{-4} \text{ mol dm}^{-3}$ $[\text{OH}^-] = 0.05 \text{ mol dm}^{-3}$ $[\text{VCH}] = 3.0 \times 10^{-3} \text{ mol dm}^{-3}$					
Ionic strength (I)			Dielectric constant (D)		
$D = 78.50$			I = 0.1 mol dm ⁻³		
$10 \times \text{I}$ (mol dm ⁻³)	$\sqrt{\text{I}}$	$10^3 \times k_{\text{obs}}$ (s ⁻¹)	D	$10^2 \times 1/D$	$10^3 \times k_{\text{obs}}$ (s ⁻¹)
0.50	0.22	1.91	78.50	1.27	1.64
1.00	0.32	1.87	75.12	1.33	1.57
2.00	0.45	1.96	71.74	1.39	1.45
3.00	0.55	1.96	68.36	1.46	1.34
4.00	0.63	1.91	64.98	1.54	1.20
6.00	0.77	1.98	61.60	1.62	1.15

dependent variable 'y'. Most sets of kinetic data approximate this situation, in as much as times of observation are more accurately measurable than the chemical or physical quantities related to reactant concentrations. The straight-line selected by the common linear regression analysis is that which

minimizes the sum of the squares of the derivations of the 'y' variable from the line. The slope 'a' and intercept 'b' parameters for the above equation can be calculated by linear regression analysis by any of several mathematically equivalent but different looking experiments.

Table 3. Effect of temperature on the oxidation of VCH by alkaline permanganate.

$$[\text{MnO}_4^-] = 2.0 \times 10^{-4} \text{ mol dm}^{-3} \quad [\text{OH}^-] = 0.05 \text{ mol dm}^{-3}$$

$$[\text{VCH}] = 3.0 \times 10^{-3} \text{ mol dm}^{-3} \quad \text{I} = 0.1 \text{ mol dm}^{-3}$$

T (K)	$10^3 \times k_{\text{obs}}$ (s ⁻¹)	$10^3 \times 1/T$ (K ⁻¹) (X)	$3 + \log k_{\text{obs}}$ (Y)	$3 + \log k_{\text{obs}}$ (Y* cal)
298	2.14	3.36	0.33	0.34
303	3.06	3.30	0.49	0.46
308	3.57	3.25	0.55	0.57
313	4.68	3.19	0.67	0.67
318	5.76	3.14	0.76	0.77

Table 4. Activation parameters for the oxidation of VCH by alkaline permanganate at 298 K.

Activation parameters	Values
E_a (kJ mol ⁻¹)	39 ± 2
ΔH^\ddagger (kJ mol ⁻¹)	36 ± 1.5
ΔS^\ddagger (J K ⁻¹ mol ⁻¹)	- 165 ± 8
ΔG^\ddagger (kJ mol ⁻¹)	86 ± 4
log A	4.0 ± 0.2

Most familiar are

$$\text{Slope: } a = \frac{n \sum xy - \sum x \sum y}{n \sum x^2 - (\sum x)^2}$$

$$\text{Intercept: } b = \frac{\sum y \sum x^2 - \sum x \sum xy}{n \sum x^2 - (\sum x)^2}$$

where ‘n’ is the number of data points and summation are for all data points in the set. These data were subjected to least square analysis and verified with experimental values. From the Arrhenius plot, log k_{obs} versus $1/T$, activation parameters were figured out (Table 4).

$$E_a = -2.303 \times R \times \text{slope}$$

The other activation parameters were calculated as follows.

The Arrhenius factor ‘A’ was calculated by,

$$\log A = \log k_{\text{obs}} + \frac{E_a}{2.303RT}$$

The entropy of activation was calculated by using the equation,

$$\log k_{\text{obs}} = \left(\frac{kT}{h} \right) e^{\Delta S^\ddagger/R} \cdot e^{-E_a/RT}$$

$$2.303 \log k_{\text{obs}} = 2.303 \log \frac{kT}{h} + \frac{\Delta S^\ddagger}{R} - \frac{E_a}{RT}$$

$$\log k_{\text{obs}} = \log \frac{kT}{h} + \frac{\Delta S^\ddagger}{2.303 R} - \frac{E_a}{2.303 RT}$$

$$\log k_{\text{obs}} = \log \frac{k}{h} + \log T + \frac{\Delta S^\ddagger}{2.303 R} - \frac{E_a}{2.303 RT}$$

$$\frac{\Delta S^\ddagger}{2.303 R} = \log k_{\text{obs}} - \log \frac{k}{h} - \log T + \frac{E_a}{2.303 RT}$$

On substituting the universal gas constant ‘R’ as 8.314 J K⁻¹ mol⁻¹, the Boltzmann constant (k) = 1.3807 × 10⁻²³ J K⁻¹ and the Plank’s constant (h) = 6.630 × 10⁻³⁴ J s.

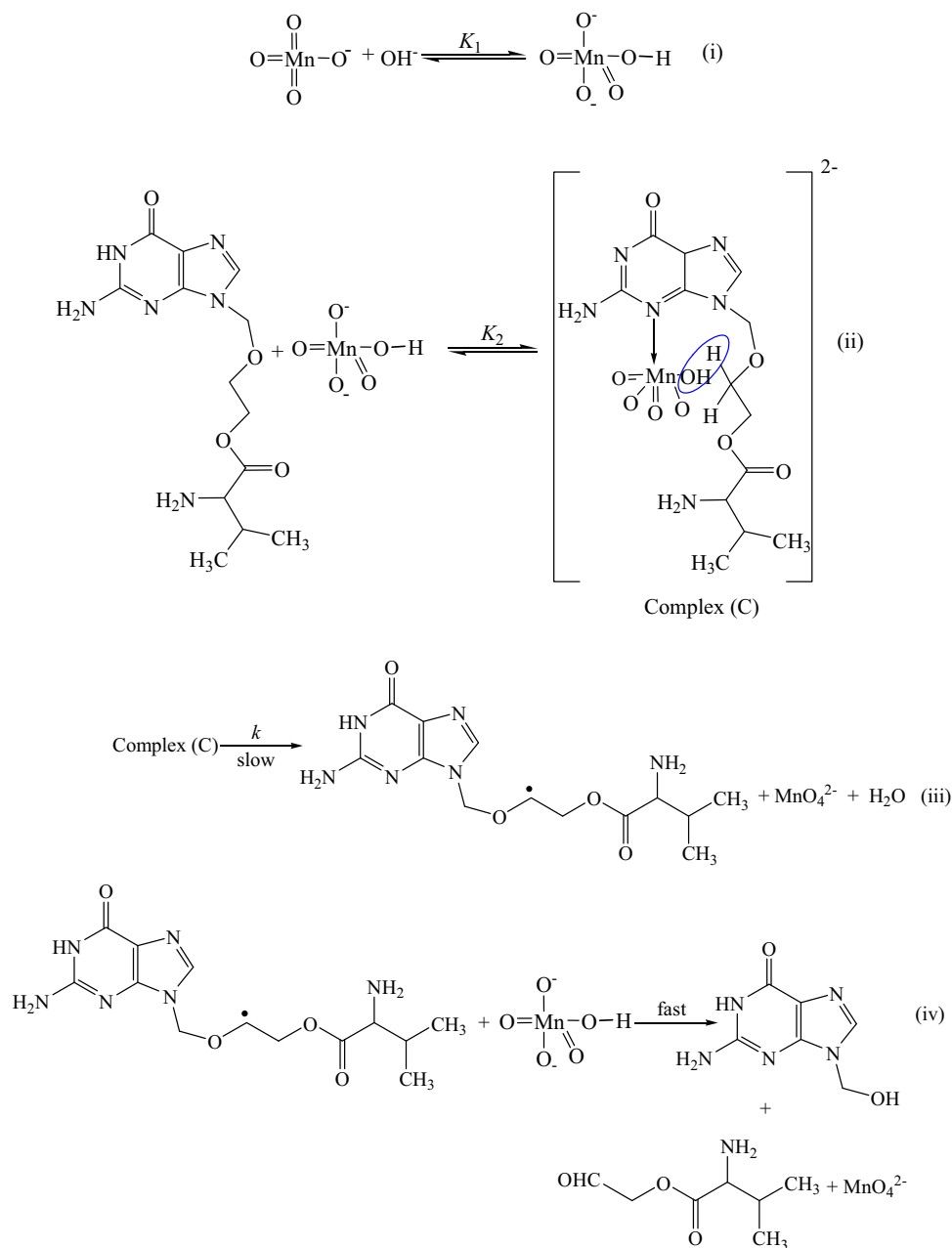
$$\frac{\Delta S^\ddagger}{2.303 \times 8.314} = \log k_{\text{obs}} - \log \frac{1.3807 \times 10^{-23}}{6.63 \times 10^{-34}} - \log T + \frac{E_a}{2.303 \times 8.314 \times T}$$

$$\frac{\Delta S^\ddagger}{19.147} = \log k_{\text{obs}} - 10.318 - \log T + \frac{E_a}{19.147T}$$

The k_{obs} should be in s⁻¹, and temperature in Kelvin, then the E_a results in J mol⁻¹ and ΔS^\ddagger in J K⁻¹ mol⁻¹. The enthalpy of activation was calculated by, $\Delta H^\ddagger = E_a - RT$ and free energy of activation from $\Delta G^\ddagger = \Delta H^\ddagger - T\Delta S^\ddagger$.

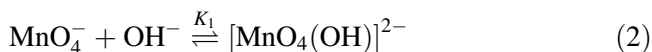
The rate constants (k) were obtained from intercept of $1/k_{\text{obs}}$ versus $1/[\text{VCH}]$ for slow step (Scheme 3). Other equilibrium constants, K_1 and K_2 were obtained from the slope and intercept of the plots, $1/k_{\text{obs}}$ versus $1/[\text{VCH}]$ and $1/[\text{OH}^-]$ (Figure 3).

In the present study, added $[\text{OH}^-]$ has a positive effect and thus combines with permanganate ion in



Scheme 3. Mechanism of oxidation of VCH by Permanganate in aqueous alkali.

alkaline medium to form alkaline permanganate ion in pre-equilibrium step as shown below. This is in accordance with the earlier work^{26,27}.



The proposed structure of MnO_4^- complex (Scheme 3) is based on the MnO_4^- oxidation of heteroaryl formamidines²⁸ in an alkaline medium. Since the progress of the reaction was monitored for change in color of oxidant, it exhibited changeover in coloration from violet to blue and then to green. Spectral

changes during the oxidation as shown in Figure 4 is evidence for the formation of MnO_4^{2-} complex by the appearance of two new bands at 432 and 608 nm followed by the disappearance of permanganate band at 526 nm.

$$[\text{MnO}_4^-] = 2.0 \times 10^{-4} \text{ mol dm}^{-3}$$

$$[\text{OH}^-] = 0.05 \text{ mol dm}^{-3}$$

$$[\text{VCH}] = 3.0 \times 10^{-3} \text{ mol dm}^{-3}$$

$$I = 0.1 \text{ mol dm}^{-3}$$

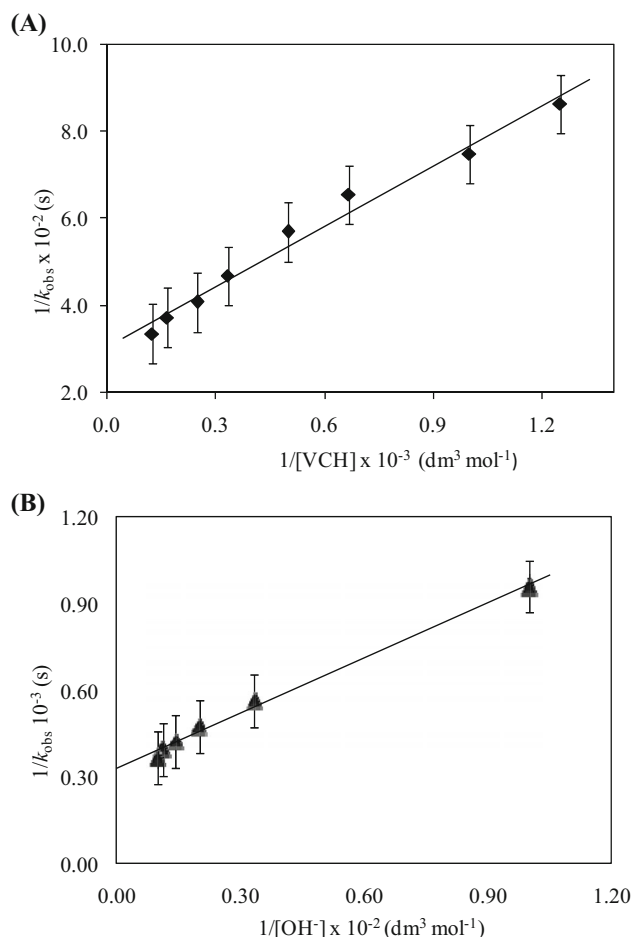


Figure 3. Verification of the rate law (eqn. 9) for oxidation of VCH by alkaline permanganate at 298 K. Plot of (A) $1/k_{\text{obs}}$ versus $1/[\text{VCH}]$ and (B) $1/k_{\text{obs}}$ versus $1/[\text{OH}^-]$ (Conditions as in Table 1).

Formation of Mn^{5+} was rejected based on the absence of absorbance at 667 nm, expected for MnO_4^{3-} . Further, the reduction of MnO_4^- is stopped^{29,30} at MnO_4^{2-} and become stable in alkali concentration maintained in this study.

The reaction with 1:2 of $[\text{VCH}]:[\text{MnO}_4^-]$ stoichiometry proceeded with pseudo-first-order dependence on $[\text{MnO}_4^-]$ and positive fractional order in both alkali and substrate concentrations. The permanganate species acts as a one-electron oxidant and affords via free radical intermediate and it is evidenced by the free radical test. The evidence for such free radical in a slow step is also reported in earlier work.^{31,32}

In the first step (1) of the proposed mechanism (Scheme 3), potassium permanganate combines with alkali to form alkali-permanganate ion $[\text{MnO}_4(\text{OH})]^{2-}$ and in succeeding step (2) the alkali-permanganate ion combines with the VCH molecule to form a complex (C). Formation of such complex (C) is confirmed

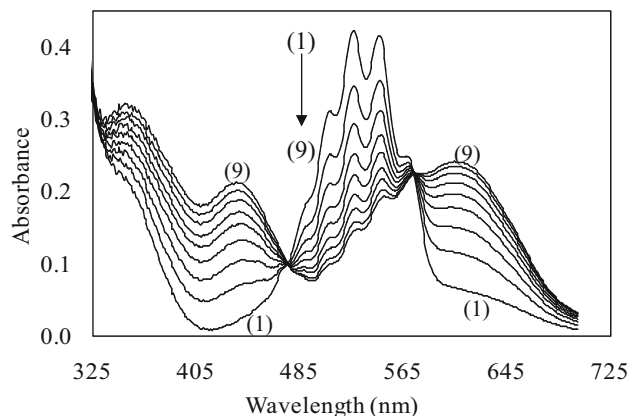


Figure 4. Spectral changes during the oxidation of VCH by alkaline permanganate with scanning time interval of: (1) 1.0, (2) 2.0, (3) 3.0, (4) 4.0, (5) 5.0, (6) 6.0, (7) 7.0, (8) 8.0, (9) 9.0 min

kinetically by Michaelis–Menten plot ($1/k_{\text{obs}}$ versus $1/[\text{VCH}]$) (Figure 3). The unstable complex (C) decomposes in a slow step to give a free radical (3) with the formation of MnO_4^{2-} . The unstable free radical as an intermediate reacts with another molecule of $[\text{MnO}_4(\text{OH})]^{2-}$ in consequent fast step (4) to yield the products 2-amino-9-(hydroxymethyl)-1H-purin-6(9H)-one and formylmethyl 2-amino-3-methyl butanoate. This was ascertained from their LC-ESI-Mass spectra, m/z peak at 159 and 181, expected for formylmethyl 2-amino-3-methylbutanoate and 2-amino-9-(hydroxymethyl)-1H-purin-6(9H)-one respectively (Figure 2). This proposed mechanism leading to the formation of aldehyde is supported by earlier studies and to quote a few, amino acid, ester, etc.³³

In the proposed mechanism (Scheme 3), complex (C) decomposes to give Mn^{6+} by abstracting an electron leading to a CH(methylene) free radical. In the next step, cleavage of alkyl oxygen (AL_2) bond rather than acyl-oxygen bond leads to an aldehyde and hydroxyl methyl purine-one. The formation of such aldehyde has been observed in the earlier reports of oxidation of amino acid ester.³³ Further, cleavage of AL_2 bond is found, leading the N- CH_2 -OH group on imidazole and is stabilized by an intramolecular hydrogen bonding.

The other possibility of direct '2' electron reduction was i.e., hypomanganate (MnO_4^{3-}) to yield a final product. Such single step oxidation was rejected as the development of $\text{Mn}^{\text{V}}\text{O}_4^{3-}$ ion was not noticed in the progress of the reaction, which was expected for the absorbance at 667 nm. Hence, it is concluded that the oxidative mechanism of VCH by alkaline permanganate follows as per Scheme 3.

According to Scheme 3,

$$\text{Rate} = kK_2[\text{MnO}_4(\text{OH})]^{2-}[\text{VCH}]_f \quad (3)$$

$$\text{Rate} = kK_1K_2[\text{MnO}_4^-]_f[\text{OH}^-]_f[\text{VCH}]_f \quad (4)$$

$$\text{Rate} = -\frac{[\text{MnO}_4^-]}{dt} = k[\text{Complex}]$$

However,

$$\begin{aligned} [\text{MnO}_4^-]_T &= [\text{MnO}_4^-]_f + [\text{MnO}_4(\text{OH})]^{2-} + [\text{Complex}] \\ &= [\text{MnO}_4^-]_f + K_1[\text{MnO}_4^-]_f[\text{OH}^-]_f \\ &\quad + K_1K_2[\text{MnO}_4^-]_f[\text{OH}^-]_f[\text{VCH}]_f \\ &= [\text{MnO}_4^-]_f \{ 1 + K_1[\text{OH}^-]_f \\ &\quad + K_1K_2[\text{OH}^-]_f[\text{VCH}]_f \} \\ [\text{MnO}_4^-]_f &= \frac{[\text{MnO}_4^-]_T}{1 + K_1[\text{OH}^-]_f + K_1K_2[\text{OH}^-]_f[\text{VCH}]_f} \end{aligned} \quad (5)$$

$$\begin{aligned} [\text{OH}^-]_T &= [\text{OH}^-]_f + [\text{MnO}_4(\text{OH})]^{2-} \\ &= [\text{OH}^-]_f + K_1[\text{MnO}_4^-]_f[\text{OH}^-]_f \\ &= [\text{OH}^-]_f \{ 1 + K_1[\text{MnO}_4^-]_f \} \\ [\text{OH}^-] &= \frac{[\text{OH}^-]_T}{1 + K_1[\text{MnO}_4^-]_f} \end{aligned}$$

At low concentration of

$$[\text{MnO}_4^-], [\text{OH}^-]_f = [\text{OH}^-]_T \quad (6)$$

$$\begin{aligned} [\text{VCH}]_T &= [\text{VCH}]_f + [\text{Complex}] \\ &= [\text{VCH}]_f + K_1K_2[\text{MnO}_4^-]_f[\text{OH}^-]_f[\text{VCH}]_f \\ &= [\text{VCH}]_f \{ 1 + K_1K_2[\text{MnO}_4^-]_f[\text{OH}^-]_f \} \\ [\text{VCH}]_f &= \frac{[\text{VCH}]_T}{1 + K_1K_2[\text{MnO}_4^-]_f[\text{OH}^-]_f} \end{aligned}$$

The term $K_1 K_2 [\text{OH}^-]_f [\text{MnO}_4^-]_f$ is neglected compared to 1 in the denominator as low concentration of MnO_4^- used.

Therefore,

$$[\text{VCH}]_f = [\text{VCH}]_T \quad (7)$$

On substituting eqns. (5), (6), and (7) in eqn. (4), eqn. (8) results

$$\text{Rate} = \frac{kK_1K_2[\text{MnO}_4^-]_T[\text{OH}^-]_T[\text{VCH}]_T}{1 + K_1[\text{OH}^-]_f + K_1K_2[\text{VCH}]_f[\text{OH}^-]_f} \quad (8)$$

For verification of rate law, the subscripts 'T' and 'f' are omitted and hence eqn. (8) becomes,

$$\frac{\text{Rate}}{[\text{MnO}_4^-]} = k_{\text{obs}} = \frac{kK_1K_2[\text{OH}^-][\text{VCH}]}{1 + K_1[\text{OH}^-] + K_1K_2[\text{VCH}][\text{OH}^-]} \quad (9)$$

Equation (9) is rearranged into eqn. (10), which is suitable for verification.

$$\frac{1}{k_{\text{obs}}} = \frac{1}{kK_1K_2[\text{OH}^-][\text{VCH}]} + \frac{1}{kK_2[\text{VCH}]} + \frac{1}{k} \quad (10)$$

The rate law (eqn. 9) has been proved by plotting of $1/k_{\text{obs}}$ versus $1/[\text{VCH}]$ and $1/[\text{OH}^-]$ which gave linear plots (Figure 3). From the slopes and intercepts of these plots, the values, $k = 3.18 \times 10^{-3} \text{ s}^{-1}$, $K_1 = 4.42 \text{ dm}^3 \text{ mol}^{-1}$, and $K_2 = 3.64 \times 10^3 \text{ dm}^3 \text{ mol}^{-1}$ for 298 K were calculated. The K_1 value obtained is in good agreement with the literature value of ($6.6 \text{ dm}^3 \text{ mol}^{-1}$).^{29,34}

Further, equilibrium constants K_1 , K_2 along with k were used to regenerate k_{obs} values for the different experimental conditions. It is found that the regenerated results are in good agreement with experimental results (Table 1). This strengthens the proposed mechanism (Scheme 3) and rate law (eqn. 9).

In the proposed mechanism (Scheme 3), the reaction takes place via complex formation (step 2). The value of ΔS^\ddagger (-165) strengthens a relatively rigid complex formation and hence its stability.³⁵ The higher negative value of ΔS^\ddagger proves that the complex is more ordered than other species present in the reaction. It is noticed in the reaction that as the dielectric constant of the media increases rate increases. This indicates that the reaction is more favorable in aqueous media.

4. Conclusions

Oxidation of VCH by alkaline permanganate proceeds through the intervention of free radicals generated from VCH (methylene moiety). The active species of permanganate is found to be $[\text{MnO}_4(\text{OH})]^{2-}$ which was formed in a prior equilibrium step of the mechanism. The mechanism occurs through a complex formed between MnO_4^- and VCH. The relatively large value of k_{obs} and small value of $\log A$ supports that the reaction was led through the inner-sphere mechanism. The overall mechanistic sequence described here is consistent with product studies and kinetic studies.

Supplementary Information (SI)

The spectrum of alkaline permanganate at 298 K, Order plot of $[\text{VCH}]$ and $[\text{OH}^-]$, Effect of dielectric

constant (D) ($\log k$ vs. $1/D$), Effect of initially added product, $[\text{MnO}_4^{2-}]$ and Arrhenius plot for the oxidation of VCH by alkaline permanganate (Figure S1–S5 and Table S1) are available at www.ias.ac.in/chemsci.

Acknowledgements

The authors are obliged to the Principal, Karnataka Science College, Dharwad, Karnataka, India for offering the essential laboratories to execute the present work.

References

- Ormrod D, Scott L J and Perry C M 2000 Valacyclovir: A review of its long term utility in the management of genital herpes simplex virus and cytomegalovirus infections *Drugs* **59** 839
- Karl R B 1995 Valacyclovir: A review of its antiviral activity, pharmacokinetic properties, and clinical efficacy *Antiviral. Res.* **28**
- Bengi U, Sibel A O and Zuhre S 2006 Electrooxidation of the antiviral drug valacyclovir and its square-wave and differential pulse voltammetric determination in pharmaceuticals and human biological fluids *Anal. Chim. Acta* **555** 341
- John J, O'Brien Deborah M and Campoli R 1989 Acyclovir an updated review of its antiviral activity, pharmacokinetic properties and therapeutic efficacy *Drugs* **37** 233
- Christopher P L, Andowski D S, David R F, Sujatha S M, Jeffrey L B, Lynda S W, Chandrasekharan R and Gordon L A 2003 Gene expression in the human intestine and correlation with oral valacyclovir pharmacokinetic parameters *J. Pharmacol. Exp. Ther.* **306** 778
- Baker V S 2021 Acyclovir for SARS-CoV-2: An Old Drug with a New Purpose *Clin. Pract.* **181**
- Rajeshwari V H, Savanur A P, Nandibewoor S T and Chimatadar S A 2010 Kinetics and mechanism of uncatalysed and ruthenium(III)-catalysed oxidation of d-panthenol by alkaline permanganate *Transit. Met. Chem.* **35** 237
- Gamal A A, Ahmed F and Refat M H 2007 Spectrophotometric evidence for the formation of short-lived hypomanganate(V) and manganate(VI) transient species during the oxidation of K-carrageenan by alkaline permanganate *Carbohydr. Res.* **342** 1382
- Simandi L I, Miklos J and Schelly Z A 1984 Short-Lived manganate(VI) and manganate(V) intermediates in the permanganate oxidation of sulfite ion *J. Am. Chem. Soc.* **106** 6866
- Timy P J, Nandibewoor S T and Tuwar S M 2005 Mechanism of oxidation of L-histidine by heptavalent manganese in alkaline medium *E-J. Chem.* **2** 75
- Griffith W P 1970 Transition metal oxo complexes *Coord. Chem. Rev.* **5** 459
- Goodman Gilman's 1985 *The Pharmacological Basis of Therapeutics* 7th edn. L S Goodman, A G Gilman, T W Rall and F Murad (Eds.) (USA: McGraw Hill Medical)
- Umesh V B 1992 *Pharmaceutical Dissolution Testing* 1st edn. (New York: Marcel Dekker) p. 437
- Andrei G, Snoeck R, Goubau P, Desmyter J and Clercq E D 1992 Comparative activity of various compounds against clinical strains of herpes simplex virus *Eur. J. Clin. Microbiol. Infect. Dis.* **11** 143
- Andrei G, Snoeck R, Reymen D, Goubau P, Desmyter J and Clercq E D 1995 Comparative activity of selected antiviral compounds against clinical isolates of varicella-zoster virus *Eur. J. Clin. Microbiol. Infect. Dis.* **14** 318
- Aswani K C H, Anil K T, Gurupadayya B M, Sloka S N and Rahul Reddy M B 2010 Novel spectrophotometric determination of valacyclovir and cefotaxime using 1, 2-naphthaquinone-4-sulfonic acid sodium in bulk and pharmaceutical dosage form *Arch. Appl. Sci. Res.* **2** 278
- Pharm-Huy C, Stathoulopoulou F, Sandouk P, Scherrmann J M, Palombo S and Girre C 1999 Rapid determination of valaciclovir and acyclovir in human biological fluids by high-performance liquid chromatography using isocratic elution *J. Chromatogr. B. Biomed. Sci. Appl.* **732** 47
- Ayhan S, Ozkan C K, Ozkan Y, Ulsu B and Ozkan S A 2003 Development and validation of an RP-HPLC method for the determination of valacyclovir in tablets and human serum and its application to drug dissolution studies *J. Liq. Chromatogr. Rel. Technol.* **26** 1755
- Gladys E G and Gordon L A 2006 Stability of valacyclovir: Implications for its oral bioavailability *Int. J. Pharm.* **317** 14
- Manish Y, Vivek U, Puran S, Sailendra G and Pranav S S 2009 Stability evaluation and sensitive determination of antiviral drug, valacyclovir and its metabolite acyclovir in human plasma by a rapid liquid chromatography-tandem mass spectrometry method *J. Chromatogr. B* **877** 680
- Devarushi U S, Shetti N P, Tuwar S M and Seetharamappa J 2017 Electrochemical oxidation and thermodynamic parameters for an anti-viral drug valacyclovir *Anal. Bioanal. Electrochem.* **9** 102
- Jeffery G H, Bassett J, Mendham J and Denney R C 1996 *Vogel's Text Book of Quantitative Chemical Analysis* 5th edn. (Essex, UK: ELBS, Longman) p. 371
- Vogel A I 1978 *A Text Book of Quantitative Inorganic Analysis* 4th edn. (New York: ELBS) p. 330
- Feigl F and Anger V 2005 *Spot Tests in Organic Analysis* Translated by Oesper R E (New Delhi: Elsevier India)
- Handbook of Chemistry and Physics* 1960 41st edn. C D Hodgman (Ed.) (Ohio: Chemical Rubber) p. 2513
- Panari R G, Chougale R B and Nandibewoor S T 1998 Oxidation of mandelic acid by alkaline potassium permanganate-A kinetic study *J. Phys. Org. Chem.* **11** 448
- De Oliveira L A, Toma H E and Giesbrecht E 1976 Kinetics of oxidation of free and coordinated dimethylsulfoxide with permanganate in aqueous solution *Inorg. Nucl. Chem. Lett.* **2** 195
- Ahmed F and Mohamed R S 2014 Kinetic and mechanistic investigations on the oxidation of N'-heteroaryl unsymmetrical formamides by

- permanganate in aqueous alkaline medium *Transit. Met. Chem.* **39** 379
29. Ladbury J W and Cullis C F 1958 Kinetics and mechanism of oxidation by permanganate *Chem. Rev.* **58** 403
30. Zordan T A and Loren G H 1968 Thermochemistry and oxidation potentials of manganese and its compounds *Chem. Rev.* **68** 737
31. Badi S S and Tuwar S M 2015 Permanganate oxidative products of moxifloxacin, a fluoroquinolone drug: A mechanistic approach *Res. Chem. Intermed.* **41** 7827
32. Angadi M A and Tuwar S M 2015 Mechanism of the oxidation of captopril by diperiodatoargentate(III) in aqueous alkali: A reaction kinetics study *J. Sol. Chem.* **44** 1844
33. Surender R V, Sethuram B and Navaneeth R T 1979 Kinetics of oxidation of some amino acids by KMnO_4 in a moderately concentrated H_2SO_4 medium in the presence and absence of Ag^+ *Int. J. Chem. Kinet.* **11** 165
34. Thabaj K A, Kulkarni S D, Chimatadar S A and Nandibewoor S T 2007 Oxidative transformation of ciprofloxacin by alkaline permanganate - A kinetic and mechanistic study *Polyhedron* **26** 4877
35. Walling C 1957 *Free Radicals in Solution* (New York: Academic Press) p.38